Intestine-specific expression of *MOGAT2* partially restores metabolic efficiency in *Mogat2*-deficient mice[S]

Yu Gao,[1] David W. Nelson,[1] Taylor Banh, Mei-I Yen, and Chi-Liang Eric Yen[2]

Department of Nutritional Sciences, University of Wisconsin, Madison, WI

Abstract **Acyl CoA:monoacylglycerol acyltransferase (MGAT) catalyzes the resynthesis of triacylglycerol, a crucial step in the absorption of dietary fat. Mice lacking the gene *Mogat2*, which codes for an MGAT highly expressed in the small intestine, are resistant to obesity and other metabolic disorders induced by high-fat feeding. Interestingly, these *Mogat2*$^{-/-}$ mice absorb normal amounts of dietary fat but exhibit a reduced rate of fat absorption, increased energy expenditure, decreased respiratory exchange ratio, and impaired metabolic efficiency. MGAT2 is expressed in tissues besides intestine. To test the hypothesis that intestinal MGAT2 enhances metabolic efficiency and promotes the storage of metabolic fuels, we introduced the human *MOGAT2* gene driven by the intestine-specific villin promoter into *Mogat2*$^{-/-}$ mice. We found that the expression of *MOGAT2* in the intestine increased intestinal MGAT activity, restored fat absorption rate, partially corrected energy expenditure, and promoted weight gain upon high-fat feeding. However, the changes in respiratory exchange ratio were not reverted, and the recoveries in metabolic efficiency and weight gain were incomplete. These data indicate that MGAT2 in the intestine plays an indispensable role in enhancing metabolic efficiency but also raise the possibility that MGAT2 in other tissues may contribute to the regulation of energy metabolism.**—Gao, Y., D. W. Nelson, T. Banh, M-I. Yen, and C-L. E. Yen. **Intestine-specific expression of *MOGAT2* partially restores metabolic efficiency in *Mogat2*-deficient mice. *J. Lipid Res.* 2013.** 54: **1644–1652.**

Supplementary key words triacylglycerol • dietary fat • neutral lipid metabolism

Acyl CoA:monoacylglycerol acyltransferase (MGAT) catalyzes the esterification of monoacylglycerol and fatty acids (in the form of acyl CoA) to generate diacylglycerol, a precursor of triacylglycerol and phospholipids (1). The enzyme plays a prominent role in the intestine, where monoacylglycerol and fatty acids resulting from the digestion of dietary triacylglycerol are resynthesized in the enterocytes. This triacylglycerol resynthesis is required for the assembly of chylomicrons, which transport the absorbed dietary fat and other lipid-soluble nutrients in the circulation (2, 3). MGAT activity has also been reported in a few other tissues of vertebrates, including liver and adipose tissues (4, 5), where its physiological roles remain to be determined. In contrast, enzymes that catalyze triacylglycerol synthesis through sequential acylation of glycerol-3-phosphate are expressed in most cells, and this alternative GPAT pathway is dominant in most tissues (6).

Three homologous genes, *Mogat1–3*, have been identified to encode MGAT enzymes in mammals (7–10). Among them, *Mogat2* is highly expressed in the intestine of both humans and rodents (8, 11). Consistent with an essential role in intestinal fat absorption, mice with the gene disrupted (*Mogat2*$^{-/-}$) are protected from obesity and other metabolic disorders induced by high-fat feeding (12). However, these mice consume and absorb normal quantities of fat. Associated with a delay in the entry of dietary fat into the circulation, *Mogat2*$^{-/-}$ mice exhibit an unexpected increase in energy expenditure, accounting for decreases in metabolic efficiency (12). Interestingly, *Mogat2*$^{-/-}$ mice exhibit increases in energy expenditure even when fed a fat-free diet, and inactivating MGAT2 in the absence of high-fat feeding also protects the hyperphagic Agouti yellow mouse from excess weight gain (13).

These findings suggest that intestinal MGAT2 regulates systemic energy metabolism but cannot rule out a role of the low levels of MGAT2 expression in other tissues, including brown and white adipose tissues (12). Indeed, in the adipose tissues of genetically identical C57Bl/6J mice, the expression levels of MGAT2 are higher in mice that gain more weight in response to high-fat feeding (14), suggesting that MGAT2 may play a functional role in that tissue. To test the hypothesis that MGAT2 in the intestine mediates triacylglycerol synthesis required for maximizing the

This work was supported by the American Heart Association (C-L.E.Y.) and National Institutes of Health Grants R01-DK-088210 (C-L.E.Y.) and T32-DK-007665 (D.W.N.).

Manuscript received December 23, 2012 and in revised form 15 March 2013.

Published, JLR Papers in Press, March 27, 2013
DOI 10.1194/jlr.M035493

Abbreviations: DAG, diacylglycerol; DGAT, diacylglycerol acyltransferase; MAG, monoacylglycerol; MGAT, monoacylglycerol acyltransferase; PL, phospholipid; RER, respiratory exchange ratio; TAG, triacylglycerol.

[1]Y. Gao and D. W. Nelson contributed equally to this work.
[2]To whom correspondence should be addressed.
e-mail: yen@nutrisci.wisc.edu

[S] The online version of this article (available at http://www.jlr.org) contains supplementary data in the form of one figure.

assimilation of dietary fat and to determine the extent to which intestinal MGAT2 contributes to metabolic efficiency, in this study we examined whether expressing MGAT2 specifically in the intestine of *Mogat2*$^{-/-}$ mice is sufficient to normalize intestinal lipid processing and systemic energy balance upon high-fat feeding.

MATERIALS AND METHODS

Mice

To generate a transgene for overexpressing MGAT2 in the intestine specifically, human MGAT2 cDNA was cloned into the p12.4kbVil plasmid containing the 12.4 kilobase regulatory elements of the villin gene (a kind gift of Dr. D. Gumucio, University of Michigan, Ann Arbor, MI), which drives high level expression within the entire intestinal epithelium of transgenic mice (15). The DNA fragments containing the villin regulatory sequences linked to MGAT2 cDNA (*vil-hMOGAT2* transgene) were released, gel purified, and injected into fertilized eggs of C57Bl/6J mice. Four male founders were crossed with C57Bl/6J mice to generate offspring, and two lines with relatively low or high expression of human *MOGAT2* mRNA were selected and named M2$^{Int\text{-}L}$ and M2$^{Int\text{-}H}$, respectively, for experiments reported in this study. *Mogat2*$^{-/-}$ mice in the C57Bl/6J genetic background were generated as reported previously (12). Male *Mogat2*$^{+/-}$ mice carrying the *hMOGAT2* transgene were crossed with female *Mogat2*$^{+/-}$ mice without the transgene to generate littermates for experimental groups of each transgenic line of mice (Wild-type, mice with endogenous *mMogat2* gene but not the *hMOGAT2* transgene; *Mogat2*$^{-/-}$, mice without either *mMogat2* or *hMOGAT2*; M2$^{Int\text{-}L}$ and M2$^{Int\text{-}H}$, mice without endogenous *mMogat2* gene but with a relative low or high level, respectively, of *hMOGAT2* expression). Wild-type and *Mogat2*$^{-/-}$mice from both lines were included in the experiments. As differences in their metabolic phenotypes were more pronounced (12), adult male mice were used for experiments. Mice were housed at 22°C on a 12 h light, 12 h dark cycle. Weighing of mice and changes of diets and cages were performed between 3 and 6 PM. All animal procedures were approved by the University of Wisconsin-Madison Animal Care and Use Committee and were conducted in conformity with the Public Health Service Policy on Humane Care and Use of Laboratory Animals.

Genotyping

To detect the presence of the transgene, a three-primer PCR was performed on genomic DNA using two forward primers 5′-GCCTTCTCCTCTAGGCTCGT-3′ (P1) and 5′-GCTTCGGAGAGTGAGTCCAT-3′ (P2) with a shared reverse primer 5′-AGGACTCCATGGGGGTGGAA-3′ (P3). The reaction produces a 625 bp amplicon and a 415 bp amplicon from endogenous mouse *Mogat2* and human *MOGAT2* cDNA, respectively (Fig. 1B). To determine the presence or absence of the mouse *Mogat2*-targeted alleles in *Mogat2*$^{-/-}$ mice, another three-primer PCR (5′-CCTTTAGCCTGGTCTAGGCAGAG-3′; 5′-CAGCAAAGCCCCCTCCTGAATCTCTC-3′; 5′-CGTTGACTCTAGAGGATCCGAC-3′) was performed as described (12).

Diets

Mice were fed a complete, fixed-formula diet (#8604, Teklad, Madison, WI). A series of semipurified (defined) diets containing 10, 45, or 60% calories from fat were used to examine the effect of replacing carbohydrate with dietary fat on food intake and energy expenditure (D12450B, D12451, and D12492, Research Diets, New Brunswick, NJ). In these diets, protein calories (from casein) were held constant at 20%, as were micronutrient and fiber contents, while fat (lard) replaced carbohydrate (corn starch and sucrose) to increase fat calories from 10 to 45 or 60%. Each diet contained 3.8, 4.7, and 5.2 kcal/g metabolizable energy, respectively (formulas are available at www.researchdiets.com).

Quantitative PCR

Tissue samples from age-matched mice fed a 60 kcal% fat diet for two months were homogenized, and total RNA was extracted and passed through gDNA Eliminator spin columns to remove genomic DNA (RNeasy Plus Mini Kit, Qiagen, Valencia, CA). RNA (2 μg) was reverse transcribed (Superscript III Supermix, Invitrogen, Grand Island, NJ), and quantitative PCR was performed with SYBR Green PCR mix (Applied Biosystems, Grand Island, NJ) and analyzed with the ABI PRISM 7000 Sequence Detection System (Applied Biosystems). Relative expression levels were calculated by the comparative C_T (cycle of threshold detection) method as outlined in the manufacturer's technical bulletin. Cyclophilin B (*Cypb*) expression was used as an internal control. The $2^{-\Delta\Delta Ct}$ method was used to calculate the fold change in gene expression (16). The primer pair used to detect both mouse and human MGAT2 mRNAs was designed to anneal to regions where the human and mouse Mogat2 cDNAs share 100% identity; the forward primer sequence is 5′-CAGAAGATCATGGGCATCTC-3′, and the reverse primer sequence is 5′-CCAAAGCTGTACTGGAAGAC-3′. The primer sequences of *Cypb* gene are 5′TGCCGGAGTCGACAATGAT-3′ (forward) and 5′-TGGAAGAGCACCAAGACAGACA-3′ (reverse).

In vitro monoacylglycerol-*O*-acyltransferase assays

MGAT activity assays were performed with total tissue homogenates as described (7). Reactions were started by adding total tissue homogenates to the assay mix and were stopped after 2 min by adding 4 ml of chloroform:methanol (2:1, v:v). The extracted lipids were dried, separated by thin-layer chromatography (TLC) on silica gel G-60 TLC plates with hexane:ethyl ether:acetic acid (80:20:1, v:v:v), and visualized with iodine vapor. Products were identified by comparison with the migration of lipid standards. The incorporation of radioactive substrates into lipid products was quantified by an imaging scanner (Typhoon FLA 7000, GE Healthcare Life Sciences, Piscataway, NJ) followed by band scraping and counting in a scintillation counter.

Synthesis of TAG in the small intestine

To examine the uptake and processing of monoacylglycerol, micelles containing radiolabeled tracers were injected into ligated intestine pouches created in anesthetized mice (17). Taurocholate micelles were prepared by resuspending dried 2-monooleoyl-rac-glycerol [^{14}C (U); ~15 Ci/mol] and unlabeled oleate with ethanol to final concentrations of 1 and 2 mM, respectively. The mixture was diluted with 20 vol of 10 mM taurocholate in PBS and rotated at 80 rpm for 1 h. Mice were fasted for 4 h. After anesthesia, a longitudinal incision was made just over the midline of the abdomen in the skin and the abdominal wall. To create an isolated pouch in the proximal intestine, a 5-0 silk suture was passed under the small intestine approximately 2 cm inferior to the pyloric sphincter of the stomach and tied off, and another suture was passed and tied off 12 cm inferior to the pyloric sphincter of the stomach. In a similar fashion, an isolated pouch in the distal intestine was created in the terminal 10 cm of the ileum adjacent to the cecum. Of the micelle preparation, 150 μl was injected into each of the pouches. Two minutes later, the proximal and the distal small intestinal pouches were excised. The luminal content was washed out and collected. Lipids from

the proximal small intestine or the distal small intestine were extracted with chloroform:methanol (2:1, v:v) and separated by TLC using a two-solvent system [first by chloroform:acetone:methanol:acetic acid:water (50:20:10:10:5) and then by hexane:ethyl ether:acetic acid (80:20:1)]. The bands corresponding to triacylglycerol (TAG), FFA, diacylglycerol (DAG), monoacylglycerol (MAG), and phospholipids (PL) were scrapped after iodine staining. Scraped silica was transferred into scintillation vials for counting of radioactivity. To verify that few radiolabeled tracers were released from the small intestine during the 2 min incubation, blood, liver, and adipose tissues were also collected and their radioactivity was measured.

Absorption of dietary fat

Fat absorption was assessed after an acute challenge of an oil bolus. Mice acclimatized to high-fat feeding for one week were fasted for 6 h and, 45 min before intragastric gavage of a bolus of oil, were injected with 500 mg/kg of the surfactant Pluronic F127 NF Prill poloxamer 407 (a gift from BASF, Florham Park, NJ) to inhibit the clearance of plasma TAG (18). To assess the rate at which dietary fat entered circulation, blood was collected before (time 0) and at indicated times after mice were challenged with 200 µl of olive oil containing 2 µCi trioleoylglycerol [carboxyl-^{14}C] for TAG measurement (Wako Diagnostics, Richmond, VA) and scintillation counting.

Metabolic phenotyping studies

A metabolic phenotyping system (LabMaster modular animal monitoring system, TSE Systems, Chesterfield, MO) with housing and wood chip bedding similar to the home-cage environment was used to continuously monitor phenotypes related to acute energy balance, including production of carbon dioxide and consumption of food, drink, and oxygen, as previously described (13). Male mice (2−3 months old) were acclimated to individual housing and metabolic cages for one week before experiments and were fed indicated diets sequentially for three days each. To examine whether there was a genotype effect on oxygen consumption (VO_2), total oxygen consumption per day, calculated by area under the curve, was plotted against baseline body weight for each mouse on each diet. In addition, VO_2 was calculated and analyzed both with and without adjusting for body weight (19–21).

Biochemical assays

Plasma triacylglycerol was measured by enzymatic assays (L-Type Triglyceride M; Wako Diagnostics) on samples collected in the afternoon after a 6 h fast. Hepatic triacylglycerol of samples collected under the same fasting condition was measured as described (22). Briefly, liver samples previously snap-frozen in liquid nitrogen were homogenized in 50 mM Tris-HCl (pH 7.4) and 250 mM sucrose. Lipids were extracted in chloroform:methanol (2:1) and separated by TLC with the solvent system hexane:ethyl ether:acetic acid (80:20:1). TAG was visualized by exposure to iodine, and TAG bands were scraped and analyzed as described using triolein as a standard. Protein concentration was measured by Pierce BCA Protein Assay Kit (Thermo, Rockford, IL). Hepatic glucose and glycogen were measured using an adapted acid hydrolysis method (23). Briefly, 40 mg of liver was homogenized in 1 ml of 1 M HCl. Half of the homogenate was neutralized with 0.5 ml of 1 M NaOH (nonhydrolyzed group). The other half was incubated at 95°C for 90 min before being neutralized with NaOH (hydrolyzed group). Glucosyl units released in both groups were measured using a colorimetric glucose kit (Wako Diagnostics). The nonhydrolyzed group represented the free glucose measurement, while the difference between the hydrolyzed and the nonhydrolyzed groups represented the glycogen measurement. Blood glucose was measured with a glucometer (One-Touch Ultra; Lifescan, Milpitas, CA). Insulin was measured by enzyme-linked immunoassay (Crystal Chem Inc., Downers Grove, IL).

Statistical analyses

All data are presented as mean ± SEM, except for indirect calorimetry data presented in Fig. 4, in which error bars were omitted to enhance clarity. Each experiment was repeated at least once to confirm reproducibility of the results. For oxygen consumption per day, differences between genotypes were assessed by the mixed-effects model with repeated measures and adjusted for body weight within the four diet strata using the PROC MIXED procedure in SAS (Cary, NC) (24). For weight patterns and glucose tolerance, differences between genotype were assessed by repeated measures ANOVA, followed by Tukey's multiple comparison test (Prism 5.01, GraphPad Inc., La Jolla, CA). For all other parameters, differences between genotypes were determined by one-way ANOVA followed by the protected least significant differences technique (Prism 5.01). $P < 0.05$ was considered statistically significant.

RESULTS

Generation of *Mogat2*$^{-/-}$ mice expressing *hMOGAT2* in the intestine

To generate mice expressing MGAT2 in an intestine-specific manner, we injected into fertilized eggs from C57Bl/6 mice a transgene linking the cDNA of human MGAT2 (*MOGAT2*) to the *cis*-regulatory element of the villin gene (**Fig. 1A**), which drives expression in all intestinal epithelia, beginning by day 12.5 postcoital and throughout life (15). Using PCR with forward primers specific to human or mouse MGAT2 genes and a shared reverse primer (Fig. 1A), we identified four founder transgenic mice (*Vil-MOGAT2*) (Fig. 1B). The presence of the transgene in the genome was also confirmed with Southern blotting (data not shown). These founders were crossed with MGAT2-targeted C57Bl/6 mice (*Mogat2*$^{-/-}$) to generate four lines of mice expressing MGAT2 only in the intestine (*Vil-MOGAT2*, *Mogat2*$^{-/-}$).

To compare the relative expression levels of human MGAT2 in the transgenic mice to those of endogenous mouse MGAT2 in the wild-type mice, we used a pair of primers annealing to the regions identical between mouse and human cDNA in the quantitative PCR analysis. Two lines of mice, referred to as M2$^{\text{Int-L}}$ and M2$^{\text{Int-H}}$, were selected for further characterization in this study, as they expressed MGAT2 mRNA at 45% and 160%, respectively, of the wild-type levels in the proximal intestine but not in other tissues, including the liver and reproductive fat pad (Fig. 1C and supplementary Fig. I). No MGAT2 mRNA was detected in *Mogat2*$^{-/-}$ mice as expected. Moderate levels of MGAT2 expression (approximately 30% that of the proximal intestine) were present in the distal small intestine of wild-type, M2$^{\text{Int-L}}$, and M2$^{\text{Int-H}}$ lines, respectively; however, the differences between these three genotypes did not reach statistical significance. Low levels of MGAT2 expression were detectable in the kidney of wild-type mice (~3% of levels found in the proximal intestine), while villin

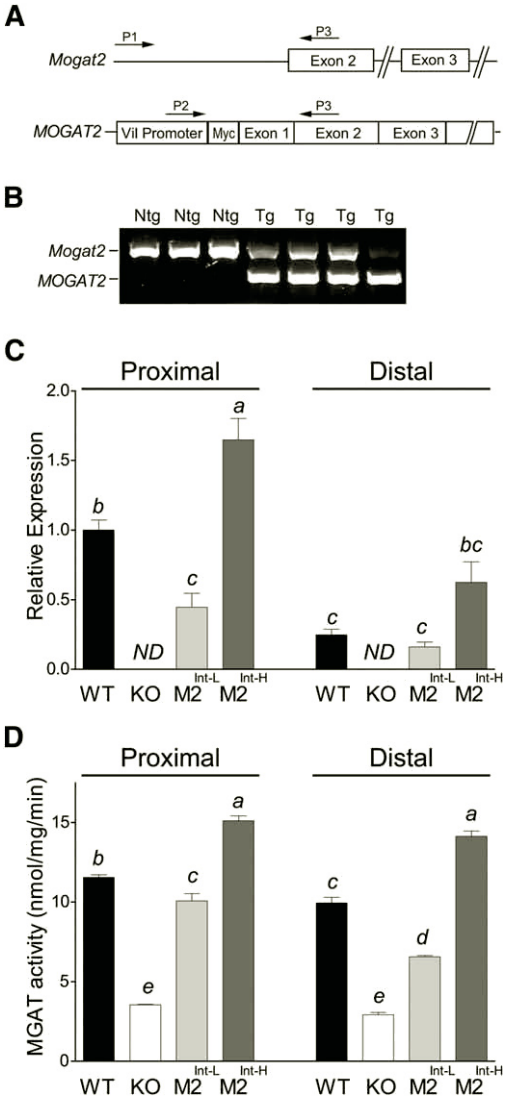

Fig. 1. Generation and characterization of mice expressing human MGAT2 in the intestine of *Mogat2*$^{-/-}$ mice. (A) Human *MOGAT2* transgene driven by villin promoter (Vil-*hMOGAT2* transgene fragment). P1, P2, and P3 are PCR primers used for genotyping. (B) Mouse endogenous *Mogat2* and human transgenic *MOGAT2* detected by a 625 bp amplicon and a 415 bp amplicon, respectively. Ntg, nontransgenic; Tg, transgenic. (C) MGAT2 mRNA levels in the proximal and distal small intestine of wild-type, *Mogat2*$^{-/-}$, M2$^{Int\text{-}L}$, and M2$^{Int\text{-}H}$ mice measured by quantitative PCR using cyclophilin as an internal control. To assess the overall expression levels of both endogenous mouse *Mogat2* and transgenic human *MOGAT2*, primers were designed annealing to identical sequences shared by mouse and human gene encoding MGAT2. *ND*, not detected. (D) MGAT activity in the proximal and distal intestine of wild-type, *Mogat2*$^{-/-}$, M2$^{Int\text{-}L}$, and M2$^{Int\text{-}H}$ mice. $n = 4-8$ per group; Bars represent mean ± SEM. Differences between bars without the same letter are statistically significant.

promoter moderately increased kidney expression in M2$^{Int\text{-}L}$ and M2$^{Int\text{-}H}$ mice (supplementary Fig. I), which has been reported in other studies (15, 25).

In in vitro acyltransferase assay, *Mogat2*$^{-/-}$ mice showed MGAT activity at around 30% of wild-type levels in both proximal and distal small intestine. This residual activity presumably came from other enzymes exhibiting MGAT activity, such as acyl CoA:diacylglycerol acyltransferase (DGAT)1 (26), which are highly expressed in the intestine. In contrast, M2$^{Int\text{-}L}$ mice showed 75% of the MGAT activity seen in wild-type mice, whereas there was a 31% increase in MGAT activity in M2$^{Int\text{-}H}$ mice compared with wild-type mice in the proximal intestine (Fig. 1D). A similar pattern of differences in MGAT activity between genotypes was also seen in the distal intestine. These data indicate that the *hMOGAT2* transgene was expressed in M2$^{Int\text{-}L}$ and M2$^{Int\text{-}H}$ mice and that the expression reinstated MGAT2 activity in the intestine of *Mogat2*$^{-/-}$ mice.

Intestinal *hMOGAT2* restores uptake and esterification of monoacylglycerol

We next examined whether expression of MGAT2 increases the ability of the intestine to take up and esterify monoacylglycerol. To avoid potential effects of gastric emptying and digestion, we directly injected micelles containing ^{14}C-monooleoylglycerol and fatty acids into ligated pouches that were created in the proximal and distal intestine. We traced the radioactivity 2 min later before any significant amount of dietary fat could be secreted from the intestine.

The levels of ^{14}C-monoacylglycerol uptake, as indicated by the sum of tracers in four lipid species recovered from the intestine segments, correlated with the levels of MGAT2 expression. For example, the uptake levels were highest in M2$^{Int\text{-}H}$, followed by wild-type, M2$^{Int\text{-}L}$, and the lowest in *Mogat2*$^{-/-}$ mice in the proximal intestine (**Fig. 2**). These uptake levels were generally higher than their counterparts in the distal intestine, with the exception of the *Mogat2*$^{-/-}$ mice where uptakes were low in both segments (Fig. 2). In each line of mice, the majority of ^{14}C-monoacylglycerol

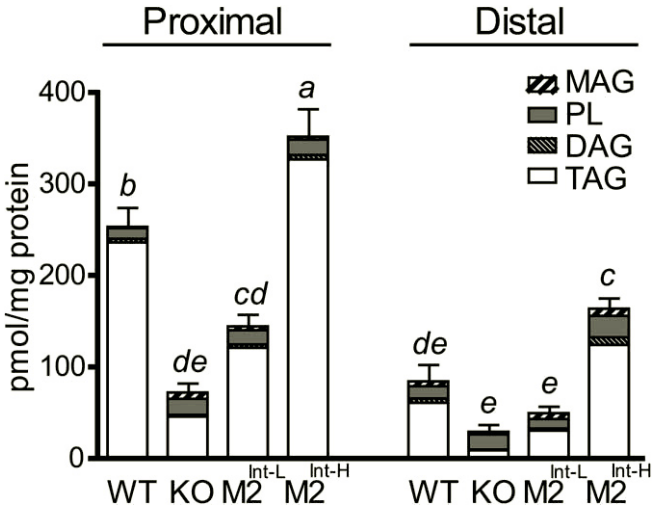

Fig. 2. Expression of human MGAT2 in the intestine of *Mogat2*$^{-/-}$ mice promotes the uptake and esterification of MAG. Micelle preparation containing fatty acids and 2-monooleoyl-rac-glycerol [^{14}C (U)] tracers were injected into ligated intestinal pouches created in the proximal and the distal intestine. Bars represent accumulation of tracers incorporated into MAG, DAG, TAG, and PL in each intestine segment of wild-type, *Mogat2*$^{-/-}$, M2$^{Int\text{-}L}$, and M2$^{Int\text{-}H}$ mice. $n = 4$ per group. Differences between bars without the same letter are statistically significant.

taken up was incorporated into triacylglycerol. In the proximal intestine of wild-type mice, we found 93.3% of recovered tracer as triacylglycerol, compared with 1.5% as diacylglycerol, 4.7% as phospholipids, and 0.5% as the tracer monoacylglycerol (Fig. 2). In *Mogat2*$^{-/-}$ mice, the production of diacylglycerol and triacylglycerol was greatly reduced compared with wild-type levels, illustrating the predominate role of intestinal MGAT2 in catalyzing the process. Expression of *hMOGAT2* increased the esterification of monoacylglycerol into di- and triacylglycerol; in M2$^{\text{Int-L}}$ mice, the esterification was partially restored to 91.4% and 51.4% of wild-type levels, respectively, in the proximal intestine, whereas in M2$^{\text{Int-H}}$ mice, the levels exceeded those of wild-type mice in both segments (Fig. 2). In contrast, the amounts of tracer incorporated into phospholipids or remaining as monoacylglycerol did not correlate with the expression levels of intestinal MGAT2. In the distal intestine, corresponding to lower levels of monoacylglycerol uptake, the percentage of tracers recovered as triacylglycerol was lower as compared with their counterpart in the proximal intestine in all genotypes. Nonetheless, the levels of radiolabeled triacylglycerol remained correlative to the levels of MGAT2 expression among genotypes.

Expression of *hMOGAT2* in the intestine restores the rate of fat absorption

Mogat2$^{-/-}$ mice absorb normal quantities of dietary fat; however, the rate of fat absorption in these mice is reduced compared with wild-type controls, as the entry of dietary fat into the circulation is delayed (12). Thus, we examined whether expressing *hMOGAT2* in the intestine increases the rate of fat absorption in *Mogat2*$^{-/-}$ mice. An intragastric bolus of olive oil containing ^{14}C-trioleoylglycerol was administered after mice were injected with a lipoprotein lipase inhibitor. The labeled dietary fat entered the circulation at a reduced rate in *Mogat2*$^{-/-}$ mice compared with wild-type mice, as expected (**Fig. 3A**). In contrast, the radioactivity increased rapidly over time in both M2$^{\text{Int-L}}$ and M2$^{\text{Int-H}}$ mice to the same extent as in wild-type mice (Fig. 3A), indicating that restoration of intestinal MGAT activity at as low as 75% of the wild-type level is sufficient to reestablish the rate of fat absorption. In all four genotypes, the majority of the radioactivity in blood was found as triacylglycerol (Fig. 3B).

Intestinal *hMOGAT2* normalizes energy expenditure but not substrate partitioning

Mogat2$^{-/-}$ mice exhibit increased energy expenditure, as evidenced by greater oxygen consumption than in wild-type mice, even when fed a low-fat diet (13). To determine whether intestinal MGAT2 is sufficient to prevent the increases in energy expenditure, wild-type, *Mogat2*$^{-/-}$, M2$^{\text{Int-L}}$, and M2$^{\text{Int-H}}$ mice were housed in metabolic chambers and fed sequentially for three days each of the three semipurified diets containing 10, 45, or 60% of calories from fat. *Mogat2*$^{-/-}$ mice indeed consumed more oxygen than wild-type mice did across the diets, with statistically significant 10, 10, and 12% increases, respectively (**Fig. 4A**). In contrast, both M2$^{\text{Int-L}}$ and M2$^{\text{Int-H}}$ mice consumed similar

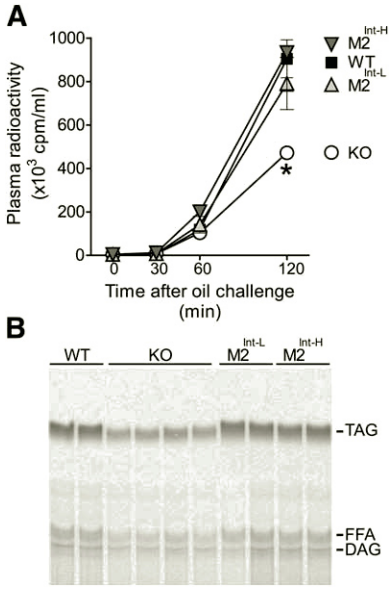

Fig. 3. Restoration of MGAT2 in the intestine of *Mogat2*$^{-/-}$ mice corrects the absorption of dietary triacylglycerol. (A) Plasma radioactivity level in mice after injection of lipase inhibitor P407 and gavage with olive oil containing trioleoylglycerol [carboxyl-^{14}C]. n = 9 for wild-type, 9 for *Mogat2*$^{-/-}$, 9 for M2$^{\text{Int-L}}$, and 5 for M2$^{\text{Int-H}}$ mice. *$P < 0.05$ versus wild-type. (B) Radiolabeled lipids extracted from plasma samples from (A) and resolved by TLC. Each lane represents a sample collected from one mouse.

levels of oxygen as wild-type mice when fed the 10% fat diet. When fed 45% or 60% high-fat diet, they both exhibited oxygen consumption levels that were intermediate between *Mogat2*$^{-/-}$ and wild-type mice, although the differences compared with either control group, decreases relative to *Mogat2*$^{-/-}$ mice and increases relative to wild-type mice, did not reach statistical significance (Fig. 4A).

Likewise, when total oxygen consumption per day was plotted against the baseline body weight of each mouse, regression lines of *Mogat2*$^{-/-}$ mice were significantly elevated relative to wild-type controls (data not shown). Based on the mixed-effects model within the three diet strata, *Mogat2*$^{-/-}$ mice consumed approximately 7–9% more oxygen than did controls across diets at any given body weight. In contrast, both M2$^{\text{Int-L}}$ and M2$^{\text{Int-H}}$ mice exhibited an intermediate phenotype, such that regression lines of each were not significantly different from that of *Mogat2*$^{-/-}$ mice or wild-type controls.

As more fat replaced carbohydrate in their diets, all four groups of mice showed the expected decreases in overall respiratory exchange ratio (RER), indicating an increased proportion of fatty acid oxidation (Fig. 4B). On the low-fat diet, their RERs rose during the night, indicating that dietary carbohydrate was a preferred energy substrate when mice were active and eating (Fig. 4B, C). Across diets, RER did not differ among groups during the dark phase of the diurnal cycle when mice were mostly in the postprandial state. In contrast, *Mogat2*$^{-/-}$ mice showed lower RER compared with wild-type mice during the day, when mice were mostly dormant and fasting (Fig. 4C). The differences in RER reached statistical significance when mice were fed

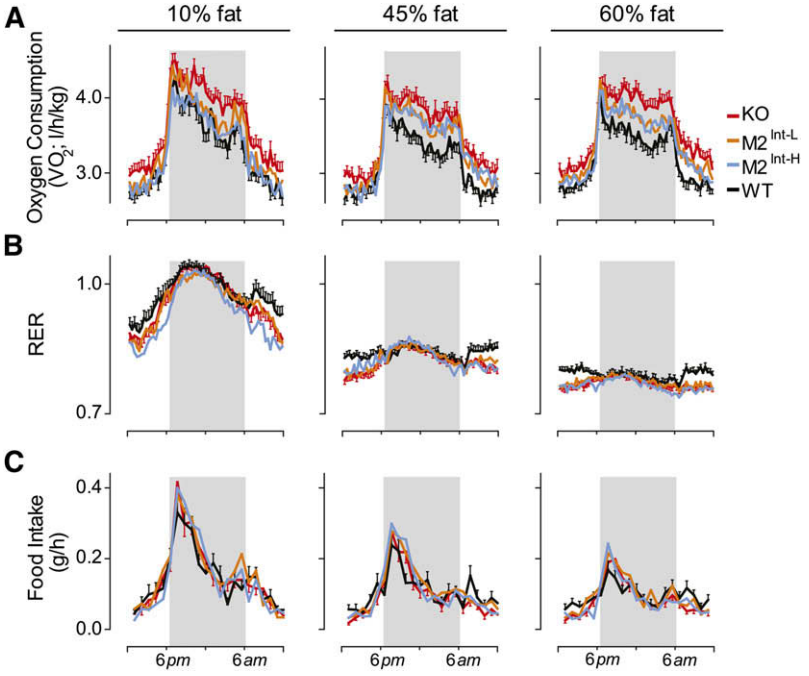

Fig. 4. Restoration of MGAT2 in the intestine partially attenuates the increased oxygen consumption but does not correct the altered respiratory exchange ratio of *Mogat2*$^{-/-}$ mice. Mice (12–14 weeks old) were fed sequentially semipurified (defined) diets containing 10, 45, or 60% calories from fat for three days per diet. (A) Oxygen consumption rates adjusted for baseline body weights of each mouse at the start of each diet treatment. (B) RERs were calculated by dividing carbon dioxide production with oxygen consumption (VCO_2/VO_2). (C) Food intake per hour. Data from each mouse were pooled from the same time of the day of the same diet treatment. Graphs represent average days. $n = 12-19$ mice per group. Gray areas mark dark phase of the light cycle (6 PM to 6 AM). Error bars for M2^{Int-L} and M2^{Int-H} mice were omitted to enhance clarity.

the high-fat diets (45 and 60 kcal%). Interestingly, despite partial normalization of oxygen consumption, both M2^{Int-L} and M2^{Int-H} mice showed RER profiles that tracked with *Mogat2*$^{-/-}$ mice, indicating that alterations in the use of carbohydrate versus fat are not corrected. The amounts of total food intake decreased in all mice when they were fed more calorie-dense, high-fat diets (Fig. 4C). However, regardless of the fat content, food intake did not differ between genotypes.

Expression of *hMOGAT2* partially restores metabolic efficiency in diet-induced weight gain

We next determined whether expressing MGAT2 only in the intestine is sufficient in promoting weight gain in response to high-fat feeding. All mice gained weight upon high-fat feeding but not to the same degree (**Fig. 5**). Whereas wild-type mice gained on average 17.3 g of body weight, *Mogat2*$^{-/-}$ mice gained only 6.5 g after 10 weeks of high-fat feeding (Fig. 5). As a result, they weighed only 75.2% as much as wild-type mice. In contrast, M2^{Int-L} and M2^{Int-H} mice gained 10.8 and 11.9 g, respectively, which was significantly more than *Mogat2*$^{-/-}$ mice but significantly less than wild-type mice (Fig. 5). Both lines of mice weighed around 88% of wild-type mice after the same duration of high-fat feeding.

After high-fat feeding, wild-type mice, but not *Mogat2*$^{-/-}$ mice, developed hepatic steatosis as indicated by increases in liver mass and triacylglycerol content (**Fig. 6A**, B). Both M2^{Int-L} and M2^{Int-H} mice showed an intermediate phenotype; their livers did not enlarge like those of wild-type mice, but their hepatic triacylglycerol concentrations were higher than that of *Mogat2*$^{-/-}$ mice. In contrast, there was no significant difference in hepatic glycogen levels among all four groups (data not shown). After high-fat feeding, wild-type mice also showed a higher level of fasting plasma insulin levels than the other three groups of mice, whereas there were no statistically significant differences in fasting blood glucose levels between them (Fig. 6C, D), consistent with the idea that wild-type mice became less sensitive to insulin. When challenged intraperitoneally with a dose of glucose, the rises in blood glucose were greater and lasted longer in wild-type mice than in the other three groups (Fig. 6D). The area under the curve of wild-type mice was 14% greater than that of *Mogat2*$^{-/-}$ mice, although the difference did not reach statistical significance. There were no differences in the response to glucose challenge between *Mogat2*$^{-/-}$, M2^{Int-L}, and M2^{Int-H} mice (Fig. 6D).

DISCUSSION

We previously reported that *Mogat2*$^{-/-}$ mice exhibit increased energy expenditure and are protected from obesity induced by diets or the agouti mutation, demonstrating a role of the MGAT2 enzyme in the efficient use and storage of metabolic energy. In this study, we report that MGAT2

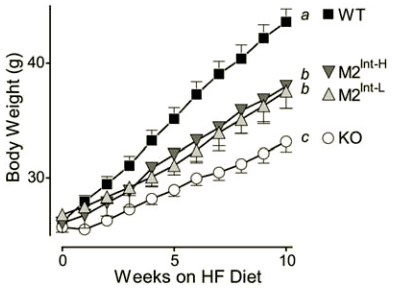

Fig. 5. Restoration of MGAT2 in the intestine partially restores metabolic efficiency in *Mogat2*$^{-/-}$ mice in response to high-fat feeding. Body weights of 12-week-old wild-type, *Mogat2*$^{-/-}$, M2^{Int-L}, and M2^{Int-H} mice were measured weekly after switching from chow to 60% diet for 10 weeks. $n = 13-26$ per group.

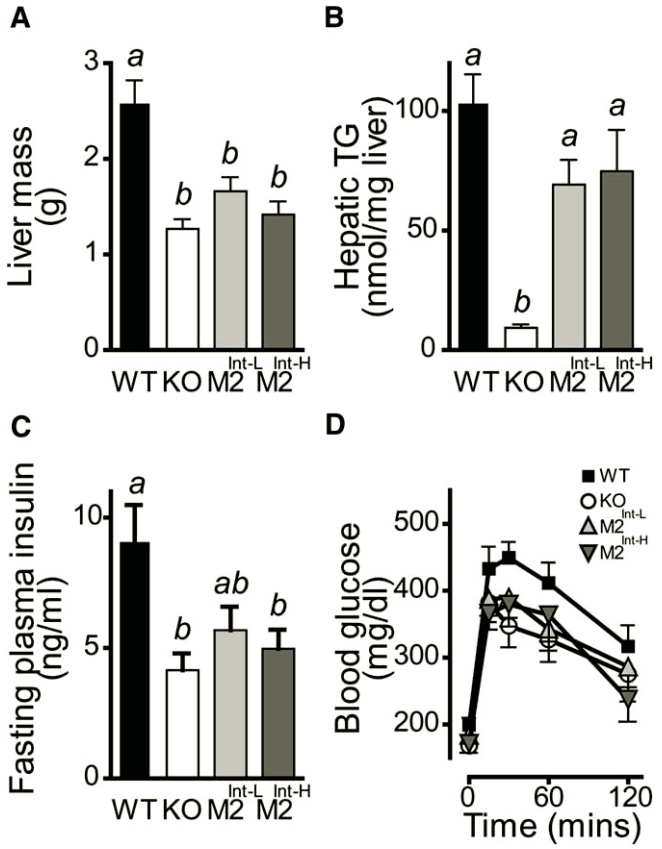

Fig. 6. Effects of restoring intestinal MGAT2 on diet-induced hepatic steatosis and glucose intolerance in *Mogat2*$^{-/-}$ mice. (A) Liver mass and (B) hepatic triacylglycerol of 6-month-old male mice fed the 60% fat diet for three months. (C) Fasting plasma insulin and (D) blood glucose concentration following an intraperitoneal glucose challenge in 5- to 6-month-old mice fed the 60% fat diet for two months. $n = 8-12$ per group; bars represent mean ± SEM. Differences between bars without the same letter are statistically significant.

in the intestine regulates the uptake and reesterification of monoacylglycerol and promotes assimilation of dietary fat into body fat in mice. MGAT2 likely serves the same biochemical and physiological functions in humans, as expressing human *MOGAT2*, specifically in the intestine of *Mogat2*$^{-/-}$ mice, increased intestinal MGAT activity, restored fat absorption, and partially corrected energy expenditure. After high-fat feeding, both lines of transgenic mice that express MGAT2 only in the intestine gained more weight than their *Mogat2*$^{-/-}$ littermates without the transgene. This finding indicates that intestinal MGAT2 is sufficient, to a significant extent, to promote efficient assimilation of dietary fat. However, these mice did not gain as much weight as their wild-type littermates, raising the possibility that the low levels of MGAT2 expressed in other tissues may also contribute to enhancing metabolic efficiency.

The best known function of MGAT activity is in the absorption of dietary fat, where MGAT catalyzes the reassembly of digested triacylglycerol (2). MGAT2 is the major contributor of MGAT activity in the intestine (8, 12). MGAT activity in vitro and the ability to incorporate monoacylglycerol into triacylglycerol were significantly reduced in the intestine of *Mogat2*$^{-/-}$ mice. They were restored proportionally to the levels of MGAT2 expression when MGAT2 was reintroduced in the intestine of M2$^{\text{Int-L}}$ and M2$^{\text{Int-H}}$ mice (Figs. 1 and 2). Earlier biochemical studies of the intestine suggested that MGAT activity produces diacylglycerol designated for triacylglycerol synthesis (27). Diacylglycerol produced in the GPAT pathway, on the other hand, is a precursor for both triacylglycerol and phospholipid synthesis (28). Consistent with these earlier reports, we found that inactivating or reintroducing MGAT2 modulated the amounts of monoacylglycerol incorporated into triacylglycerol (Fig. 2). In contrast, MGAT2 expression did not significantly affect the levels of radioactivity detected in phospholipids, whose production was likely mediated by the GPAT pathway. That the diacylglycerols generated from these two pathways did not enter the same pool is in keeping with the idea that lipid metabolizing enzymes interact with specific partners to channel lipid substrates toward different fates.

Our data suggest that MGAT2 controls the rate of monoacylglycerol uptake by the intestine, as the levels of MGAT2 expression determine the cumulative levels of all lipids derived from the ^{14}C-monoacylglycerol tracer in the intestine. By injecting substrates directly into the intestinal pouches, these results demonstrated that the decreased lipid uptake is a cell-autonomous event due to the absence of MGAT2 in the enterocytes rather than a consequence of systemic effects, such as delayed gastric emptying, which has been reported in *Mogat2*$^{-/-}$ mice (12). In wild-type mice, we found more tracer was taken up in the proximal intestine, where MGAT2 expression is higher, than in the distal intestine (Fig. 2). The rest of the tracer remained in the corresponding lumen (data not shown). In *Mogat2*$^{-/-}$ mice, the amounts of tracer taken up were low in both sections, with more pronounced difference from the wild-type mice in the proximal intestine. Expression of *MOGAT2* increased the monoacylglycerol uptake, and the levels of expression correlated with the levels of the uptake in both M2$^{\text{Int-L}}$ and M2$^{\text{Int-H}}$ mice. In contrast, the uptake and distribution of radiolabeled fatty acids were not different between wild-type and *Mogat2*$^{-/-}$ mice (data not shown), consistent with an intact GPAT pathway in these mice. The mechanism for monoacylglycerol uptake in the intestine remains unclear. A transporter for monoacylglycerol, likely shared with fatty acids, has been proposed, as the uptake of monoacylglycerol is saturable and is hindered by excess fatty acids (29). Our data suggest that MGAT2 may facilitate uptake by esterifying monoacylglycerol, analogous to how long-chain fatty acyl CoA synthetases facilitate fatty acid uptake.

Consistent with reduced monoacylglycerol uptake and esterification in the intestine, deficiency of MGAT2 delays the entry of dietary fat into circulation. Reintroducing MGAT2 in the intestine corrected it (Fig. 3). Both M2$^{\text{Int-L}}$ and M2$^{\text{Int-H}}$ mice show rates of fat absorption similar to wild-type mice, despite their differences in the levels of intestinal MGAT activity. This finding suggests that MGAT activity at 75% of wild-type levels as exhibited in M2$^{\text{Int-L}}$ mice was sufficient to facilitate fat absorption. Additional

MGAT activity in $M2^{Int\text{-}H}$ mice did not confer a higher rate of fat absorption, as other steps in the formation and secretion of chylomicrons may become limiting. It remains to be determined whether MGAT2 regulates the size and/or composition of chylomicrons, which may in turn modulate lipid and energy metabolism.

The importance of intestinal MGAT2 in systemic energy balance was illustrated by our findings that expressing *MOGAT2* in the intestine is sufficient to rescue metabolic efficiency and promote positive energy balance in *Mogat2*$^{-/-}$ mice. Human MGAT2 shares 81% identity in amino acid sequences with mouse enzyme and, in our studies, carried out similar biochemical and physiological functions to compensate for the mouse enzyme. Thus, MGAT2 likely serves similar physiological functions and enhances metabolic efficiency in humans. Both $M2^{Int\text{-}L}$ and $M2^{Int\text{-}H}$ mice exhibited a similar reduction in energy expenditure and increases in weight gain in response to high-fat feeding compared with *Mogat2*$^{-/-}$ mice. However, these recoveries did not reach the wild-type levels and thus appeared to be incomplete. It is possible that human MGAT2 cannot fully substitute for the functions of mouse MGAT2. Likewise, we cannot exclude the possibility that the expression pattern, both location and timing, driven by the villin *cis*-regulatory element differs from endogenous expression of MGAT2 functionally in our study. Because of our findings with indirect calorimetry, we postulate that the incomplete recovery implicates MGAT2 expressed in the extra-intestinal tissues in regulating metabolic efficiency. We noted that energy expenditure differences were more pronounced during the postprandial state when nutrients are being processed through the intestine; in contrast, the differences in the RER (and thus the relative uses of carbohydrates versus fatty acids) were more pronounced during the postabsorptive state when absorption of nutrients is complete. Both $M2^{Int\text{-}L}$ and $M2^{Int\text{-}H}$ mice showed RER profiles that tracked with *Mogat2*$^{-/-}$ mice. This finding suggests that they too have alterations in substrate partitioning compared with wild-type mice and that their extra-intestinal tissues may have altered energy metabolism like *Mogat2*$^{-/-}$ mice, leading to partial metabolic inefficiency.

The energy balance phenotypes of *Mogat2*$^{-/-}$ mice are in many aspects similar to mice deficient in DGAT1, one of the two known DGAT enzymes catalyzing the final step of triacylglycerol synthesis (30–32). Also associated with a reduction in rate but normal quantity of fat absorption (33), *Dgat1*$^{-/-}$ mice exhibit increased energy expenditure, impaired metabolic efficiency, and resistance to obesity. They are also protected from hepatic steatosis and other metabolic disorders linked to obesity. DGAT1 is highly expressed in the intestine and other tissues, including the adipose tissues. Reintroduction of intestinal DGAT1 using the same villin promoter as used in our study restores the rate of fat absorption and susceptibility to diet-induced hepatic steatosis and obesity, highlighting the role of intestinal lipid metabolism in systemic energy balance (34). Several inhibitors of DGAT1 have been shown to blunt postprandial increases in plasma triacylglycerol in both humans and rodents. Their effects on preventing weight gain induced by high-fat feeding have been reported in rodents (35–37). Whether some of the inhibitors are efficacious therapeutic agents for metabolic diseases in humans remains to be determined.

In this study, we showed that expressing human MGAT2 in the intestine of *Mogat2*$^{-/-}$ mice is sufficient to enhance metabolic efficiency, providing further evidence that MGAT2-mediated triacylglycerol metabolism in the intestine controls fat absorption and systemic energy balance and that the human enzyme may serve the same functions. These findings raise the prospect of inhibiting MGAT2 in the intestine as an approach to prevent or treat obesity. In addition, we found that reinstituting intestinal MGAT activity only partially restores metabolic efficiency and does not correct substrate partitioning in *Mogat2*$^{-/-}$ mice, raising the possibility that MGAT2 in other tissues may play a functional role in the use and storage of energy substrates.

The authors thank Bao Le and Adela Stieve for technical assistance in PCR assays and mouse husbandry.

REFERENCES

1. Bell, R. M., and R. A. Coleman. 1980. Enzymes of glycerolipid synthesis in eukaryotes. *Annu. Rev. Biochem.* **49:** 459–487.
2. Mansbach, C. M., and S. A. Siddiqi. 2010. The biogenesis of chylomicrons. *Annu. Rev. Physiol.* **72:** 315–333.
3. Kayden, H. J., J. R. Senior, and F. H. Mattson. 1967. Monoglyceride pathway of fat absorption on man. *J. Clin. Invest.* **46:** 1695–1703.
4. Schultz, F. M., and J. M. Johnston. 1971. The synthesis of higher glycerides via the monoglyceride pathway in hamster adipose tissue. *J. Lipid Res.* **12:** 132–138.
5. Coleman, R. A., and E. B. Haynes. 1984. Hepatic monoacylglycerol acyltransferase - characterization of an activity associated with the suckling period in rats. *J. Biol. Chem.* **259:** 8934–8938.
6. Coleman, R. A., and D. G. Mashek. 2011. Mammalian triacylglycerol metabolism: synthesis, lipolysis, and signaling. *Chem. Rev.* **111:** 6359–6386.
7. Yen, C-L. E., S. J. Stone, S. Cases, P. Zhou, and R. V. Farese, Jr. 2002. Identification of a gene encoding MGAT1, a monoacylglylcerol acyltransferase. *Proc. Natl. Acad. Sci. USA.* **99:** 8512–8517.
8. Yen, C. L., and R. V. Farese, Jr. 2003. MGAT2, a monoacylglycerol acyltransferase expressed in the small intestine. *J. Biol. Chem.* **278:** 18532–18537.
9. Cao, J., J. Lockwood, P. Burn, and Y. Shi. 2003. Cloning and functional characterization of a mouse intestinal acyl-CoA:monoacylglycerol acyltransferase, MGAT2. *J. Biol. Chem.* **278:** 13860–13866.
10. Cheng, D., T. C. Nelson, J. Chen, S. G. Walker, J. Wardwell-Swanson, R. Meegalla, R. Taub, J. T. Billheimer, M. Ramaker, and J. N. Feder. 2003. Identification of acyl coenzyme A:monoacylglycerol acyltransferase 3, an intestinal specific enzyme implicated in dietary fat absorption. *J. Biol. Chem.* **278:** 13611–13614.
11. Cao, J., P. Burn, and Y. Shi. 2003. Properties of the mouse intestinal acyl-CoA:monoacylglycerol acyltransferase, MGAT2. *J. Biol. Chem.* **278:** 25657–25663.
12. Yen, C. L., M. L. Cheong, C. Grueter, P. Zhou, J. Moriwaki, J. S. Wong, B. Hubbard, S. Marmor, and R. V. Farese, Jr. 2009. Deficiency of the intestinal enzyme acyl CoA:monoacylglycerol acyltransferase-2 protects mice from metabolic disorders induced by high-fat feeding. *Nat. Med.* **15:** 442–446.
13. Nelson, D. W., Y. Gao, N. M. Spencer, T. Banh, and C. L. Yen. 2011. Deficiency of MGAT2 increases energy expenditure without high-fat feeding and protects genetically obese mice from excessive weight gain. *J. Lipid Res.* **52:** 1723–1732.
14. Koza, R. A., L. Nikonova, J. Hogan, J. S. Rim, T. Mendoza, C. Faulk, J. Skaf, and L. P. Kozak. 2006. Changes in gene expression foreshadow diet-induced obesity in genetically identical mice. *PLoS Genet.* **2:** e81.

15. Madison, B. B., L. Dunbar, X. T. Qiao, K. Braunstein, E. Braunstein, and D. L. Gumucio. 2002. Cis elements of the villin gene control expression in restricted domains of the vertical (crypt) and horizontal (duodenum, cecum) axes of the intestine. *J. Biol. Chem.* **277:** 33275–33283.
16. Livak, K. J., and T. D. Schmittgen. 2001. Analysis of relative gene expression data using real-time quantitative PCR and the 2(-Delta Delta C(T)) method. *Methods.* **25:** 402–408.
17. Ho, S. Y., L. Delgado, and J. Storch. 2002. Monoacylglycerol metabolism in human intestinal Caco-2 cells: evidence for metabolic compartmentation and hydrolysis. *J. Biol. Chem.* **277:** 1816–1823.
18. Millar, J. S., D. A. Cromley, M. G. McCoy, D. J. Rader, and J. T. Billheimer. 2005. Determining hepatic triglyceride production in mice: comparison of poloxamer 407 with Triton WR-1339. *J. Lipid Res.* **46:** 2023–2028.
19. Butler, A. A., and L. P. Kozak. 2010. A recurring problem with the analysis of energy expenditure in genetic models expressing lean and obese phenotypes. *Diabetes.* **59:** 323–329.
20. Kaiyala, K. J., G. J. Morton, B. G. Leroux, K. Ogimoto, B. Wisse, and M. W. Schwartz. 2010. Identification of body fat mass as a major determinant of metabolic rate in mice. *Diabetes.* **59:** 1657–1666.
21. MacLean, P. S. 2011. Comment on Kaiyala et al. (2010) Identification of body fat mass as a major determinant of metabolic rate in mice. Diabetes;59:1657–1666. *Diabetes.* **60:** e3; author reply e4.
22. Snyder, F., and N. Stephens. 1959. A simplified spectrophotometric determination of ester groups in lipids. *Biochim. Biophys. Acta.* **34:** 244–245.
23. Passonneau, J. V., and V. R. Lauderdale. 1974. A comparison of three methods of glycogen measurement in tissues. *Anal. Biochem.* **60:** 405–412.
24. Zar, J. 1996. Biostatistical Analysis. 3rd edition. Prentice Hall, Upper Saddle River.
25. Pinto, D., S. Robine, F. Jaisser, F. E. El Marjou, and D. Louvard. 1999. Regulatory sequences of the mouse villin gene that efficiently drive transgenic expression in immature and differentiated epithelial cells of small and large intestines. *J. Biol. Chem.* **274:** 6476–6482.
26. Yen, C. L., M. Monetti, B. J. Burri, and R. V. Farese, Jr. 2005. The triacylglycerol synthesis enzyme DGAT1 also catalyzes the synthesis of diacylglycerols, waxes, and retinyl esters. *J. Lipid Res.* **46:** 1502–1511.
27. Johnston, J. M., G. A. Rao, and P. A. Lowe. 1967. The separation of the alpha-glycerophosphate and monoglyceride pathways in the intestinal biosynthesis of triglycerides. *Biochim. Biophys. Acta.* **137:** 578–580.
28. Kennedy, E. P. 1957. Metabolism of lipides. *Annu. Rev. Biochem.* **26:** 119–148.
29. Ho, S. Y., and J. Storch. 2001. Common mechanisms of monoacylglycerol and fatty acid uptake by human intestinal Caco-2 cells. *Am. J. Physiol. Cell Physiol.* **281:** C1106–C1117.
30. Yen, C. L., S. J. Stone, S. Koliwad, C. Harris, and R. V. Farese, Jr. 2008. Thematic review series: glycerolipids. DGAT enzymes and triacylglycerol biosynthesis. *J. Lipid Res.* **49:** 2283–2301.
31. Cases, S., S. J. Smith, Y. W. Zheng, H. M. Myers, S. R. Lear, E. Sande, S. Novak, C. Collins, C. B. Welch, A. J. Lusis, et al. 1998. Identification of a gene encoding an acyl CoA:diacylglycerol acyltransferase, a key enzyme in triacylglycerol synthesis. *Proc. Natl. Acad. Sci. USA.* **95:** 13018–13023.
32. Smith, S. J., S. Cases, D. R. Jensen, H. C. Chen, E. Sande, B. Tow, D. A. Sanan, J. Raber, R. H. Eckel, and R. V. Farese. 2000. Obesity resistance and multiple mechanisms of triglyceride synthesis in mice lacking Dgat. *Nat. Genet.* **25:** 87–90.
33. Buhman, K. K., S. J. Smith, S. J. Stone, J. J. Repa, J. S. Wong, F. F. Knapp, Jr., B. J. Burri, R. L. Hamilton, N. A. Abumrad, and R. V. Farese, Jr. 2002. DGAT1 is not essential for intestinal triacylglycerol absorption or chylomicron synthesis. *J. Biol. Chem.* **277:** 25474–25479.
34. Lee, B., A. M. Fast, J. Zhu, J. X. Cheng, and K. K. Buhman. 2010. Intestine-specific expression of acyl CoA:diacylglycerol acyltransferase 1 reverses resistance to diet-induced hepatic steatosis and obesity in Dgat1-/- mice. *J. Lipid Res.* **51:** 1770–1780.
35. Denison, H., C. Nilsson, M. Kujacic, L. Lofgren, C. Karlsson, M. Knutsson, and J. W. Eriksson. 2013. Proof of mechanism for the DGAT1 inhibitor AZD7687: results from a first-time-in-human single-dose study. *Diabetes Obes. Metab.* **15:** 136–143.
36. Cao, J., Y. Zhou, H. Peng, X. Huang, S. Stahler, V. Suri, A. Qadri, T. Gareski, J. Jones, S. Hahm, et al. 2011. Targeting Acyl-CoA:diacylglycerol acyltransferase 1 (DGAT1) with small molecule inhibitors for the treatment of metabolic diseases. *J. Biol. Chem.* **286:** 41838–41851.
37. Ables, G. P., K. J. Yang, S. Vogel, A. Hernandez-Ono, S. Yu, J. J. Yuen, S. Birtles, L. K. Buckett, A. V. Turnbull, I. J. Goldberg, et al. 2012. Intestinal DGAT1 deficiency reduces postprandial triglyceride and retinyl ester excursions by inhibiting chylomicron secretion and delaying gastric emptying. *J. Lipid Res.* **53:** 2364–2379.